Int J Adv Manuf Technol (2013) 67:1959–1966
DOI 10.1007/s00170-012-4622-1

ORIGINAL ARTICLE

Failure mechanisms of a PCD tool in high-speed face milling of Ti–6Al–4V alloy

Anhai Li · Jun Zhao · Dong Wang · Jiabang Zhao · Yongwang Dong

Received: 26 April 2012 / Accepted: 5 November 2012 / Published online: 20 November 2012

Abstract High-speed milling tests were carried out on Ti–6Al–4V titanium alloy with a polycrystalline diamond (PCD) tool. Tool wear morphologies were observed and examined with a digital microscope. The main tool failure mechanisms were discussed and analyzed utilizing scanning electron microscope, and the element distribution of the failed tool surface was detected using energy dispersive spectroscopy. Results showed that tool flank wear rate increased with the increase in cutting speed. The PCD tool is suitable for machining of Ti–6Al–4V titanium alloy with a cutting speed around 250 m/min. The PCD tool exhibited relatively serious chipping and spalling at cutting speed higher than 375 m/min, within further increasing of the cutting speed the flank wear and breakage increased greatly as a result of the enhanced thermal–mechanical impacts. In addition, the PCD tool could hardly work at cutting speed of 1,000 m/min due to the catastrophic fracture of the cutting edge and intense flank wear. There was evidence of workpiece material adhesion on the tool rake face and flank face in very close proximity to the cutting edge rather than on the chipped or flaked surface, which thereby leads to the accelerating flank wear. The failure mechanisms of PCD tool in high-speed wet milling of Ti–6Al–4V titanium alloy were mainly premature breakage and synergistic interaction among adhesive wear and abrasive wear.

Keywords Tool wear · Titanium alloy · High-speed milling · Polycrystalline diamond (PCD) inserts

A. Li · J. Zhao (✉) · D. Wang · J. Zhao · Y. Dong
Key Laboratory of High Efficiency and Clean Mechanical Manufacture of MOE, School of Mechanical Engineering, Shandong University, 17923 Jingshi Road, Jinan 250061, People's Republic of China
e-mail: zhaojun@sdu.edu.cn

A. Li
e-mail: liahsea@163.com

1 Introduction

Application of titanium alloys in the aerospace and automotive industries has received great attention from many industrialists and researchers due to their attractive properties such as high specific strength (strength-to-weight ratio) maintained at elevated temperature, superior fracture-resistant characteristics, and exceptional resistance to corrosion [1–3]. However, titanium alloys are known as difficult-to-machine materials, and machining of titanium alloys has been an issue that needs to be improved [4, 5]. Specifically, Ti–6Al–4V alloy has low elasticity modulus and exhibits severe plastic deformation, severe tool wear, and tool breakage in high-speed machining. On the other hand, this important alloy is characterized by low thermal conductivity in combination with high chemical reactivity with tool materials, leading to increased tool cutting loads and temperatures, as well as to extreme abrasion [6, 7]. High chemical reactivity of titanium at high-evaluated temperatures, especially with titanium-based tools or coatings, limits their application during machining.

For the purpose of predicting of tool wear and tool life in a fundamental way, an in-depth understanding of tool wear mechanisms is firstly required. Many researchers have investigated the wear mechanisms of cemented carbide tools when machining Ti–6Al–4V alloy [6–12]. During the machining of titanium alloy using carbide tools, the cutting tools come out to failure rapidly because of the high cutting temperature and severe adhesion between the tool and the work material [6, 7]. However, although cemented carbides exhibited good mechanical fatigue behavior [13], the carbide tools cannot be used at high cutting speed, since the tool fails due to dynamic normal component of cutting force that acts on the very small contact area of tool and high cutting temperature, leading to intensive diffusion and superficial plastic deformation, causing catastrophic failure of

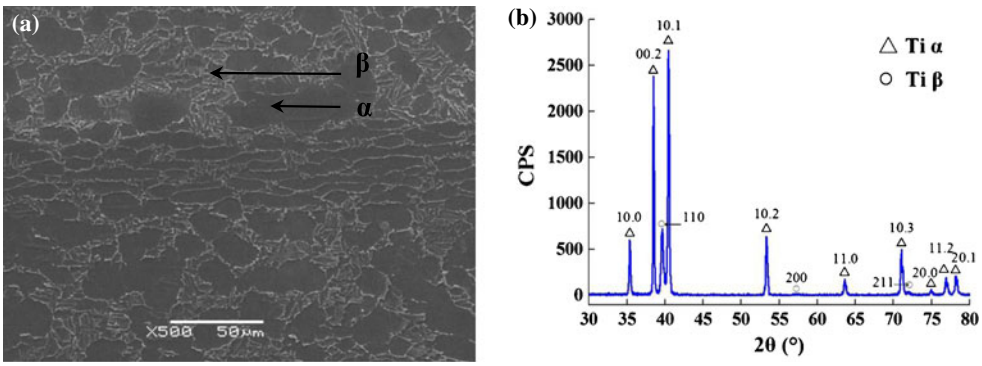

Fig. 1 Microstructure (**a**) and XRD pattern (**b**) of Ti–6Al–4V alloy

the tool [14]. Needless to say that tools which show less reactivity with titanium and has higher thermal conductivity should be used in high-speed milling operations. Due to the high hardness, high compressive strength, and excellent thermal conductivity and wear resistance, PCD has been receiving growing attention and wide applications in cutting tools [15]. Moreover, it is capable of achieving an excellent surface finish and machining efficiency when machining titanium alloys. At higher cutting speed, chemical and mechanical properties of Ti–6Al–4V cause complex wear mechanisms such as adhesion and diffusion, and PCD is firstly recommended to high-speed applications [12]. In applications where surface finish and minimal tool changes are important considerations, PCD is being increasingly employed [16]. Different failure mechanisms such as abrasion, adhesion, micro cracking, and fatigue have all been used to explain the flank wear of PCD tools [12–17]. However, there are few investigations on failure mechanisms of PCD tools in high-speed milling of titanium alloys.

The objective is to carry out high-speed milling tests using PCD tools in order to discover the wear mechanisms of the PCD tools and understand their wear behavior with respect to the high-speed cutting speed ranges.

2 Experimental methodologies

The workpiece material used in the machining test was Ti–6Al–4V alloy (solution treated and aged). Ti–6Al–4V alloy is a two-phase ($\alpha+\beta$) titanium alloy, composed of equiaxed Ti α grains (hcp) surrounded by Ti β grains (fcc), as can be seen in the typical microstructure shown in Fig. 1 (dark grains correspond to Ti α and light grains to β phase). And a rectangular block of this material with a dimension of 100×35×35 mm was selected. The chemical composition of Ti–6Al–4V alloy confirms to be the following specification (in weight percent): 5.6 % Al, 3.86 %V, 0.18 % Fe, <0.01 % Si, 0.02 % C, 0.023 %N, <0.01 %H, 0.17 % O, and balance titanium. The thermo-mechanical properties of the material are given in Table 1. It is important to note that its low thermal conductivity and its very high heat capacity may cause difficulties in heat dissipation during the cutting. Another significant characteristic of Ti–6Al–4V alloy is a very high chemical reactivity.

The geometry of the milling cutter is given in Fig. 2. The cutting tool holder used in the experiment was a 125-mm-diameter end mill (catalog number: R220.53-0125-09-8C) with a tool diameter of 125 mm, a 45° major cutting edge angle, a 10° cutting rake angle, a 20° axial rake angle, and a −5° radial rake angle made by SECO Inc. To avoid the influence of the tool tip run-out on the machined surface and tool wear analysis, only one insert was mounted on the cutter. The polycrystalline diamond (PCD) tool insert used is SEEX09T3AFFN-L1, PCD05. The polycrystalline diamond, with an average particle size of 1 μm, is embedded in a cemented tungsten carbide substrate. The insert itself is a square-shaped end milling insert with a cutting edge length of 9.525 mm, a width of 3.97 mm, a 12° rake angle, a 20° clearance angle, and a 45° side cutting edge angle.

The machine used for the milling tests was a CNC vertical machining center (Daewoo Ace-V500), equipped with variable spindle speed from 80 to 10,000 rpm, and a 15-kW motor drive. The feed direction is in the 35-mm-length direction in the 100×35-mm surface. The workpiece

Table 1 Thermo-mechanical properties of titanium alloy Ti–6Al–4V

Density (kg/m^3)	Hardness (HRC)	Elastic modulus E (GPa)	Poisson's ratio ν	Melting temperature (°C)	Thermal conductivity (W/(mK))	Heat capacity (J/(kgK))	Yield strength (MPa)	Tensile strength (MPa)
4,430	36	114	0.33	1,668	6.7	522.5	834	932

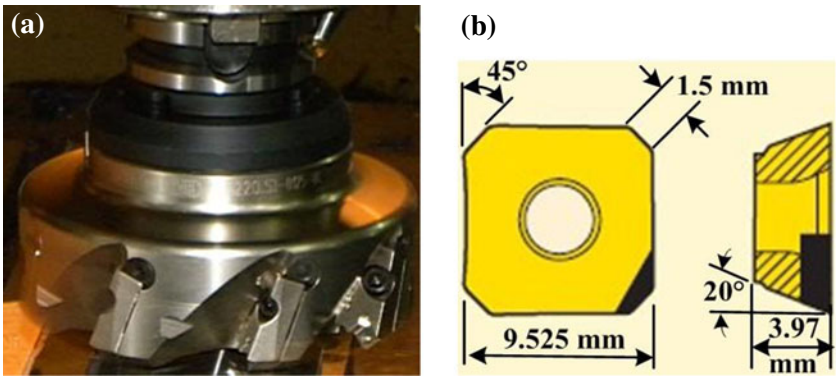

Fig. 2 The geometry of the milling cutter. **a** Tool holder. **b** Geometric dimensions of tool insert

was mounted on a specially designed fixture. The machining tests were carried out in the type of down milling operation, and wet cutting with water-soluble cutting fluid. Six different cutting speeds: 250, 375, 500, 625, 750, and 1,000 m/min were used for the PCD inserts in the milling tests. Feed per tooth was 0.05 mm/z and axial depth of cut was 0.5 mm. One fifth immersion of the cutter was employed (i.e., radial depth of cut was 25 mm). At the beginning of the experiments, to ensure measurement repeatability and fair comparison, a new sharp tool insert was mounted onto the tool holder, the machined surface (with a dimension of 35×25 mm) was milled, and the insert was marked corresponding to the experiment number for the following measurements. Machining experiments at each condition were repeated till consistencies of the experimental values are obtained.

The tool wear morphologies were firstly examined with an AM413ZT Dino-Lite digital microscope (AnMo Co., Taiwan) and dominant failure modes and failure mechanisms was analyzed by using type Quanta FEG 250 field-emission scanning electron microscope (SEM; FEI Ltd., USA) equipped with type X-MAX50 energy dispersive spectroscopy (EDS; Oxford Ltd., Britain).

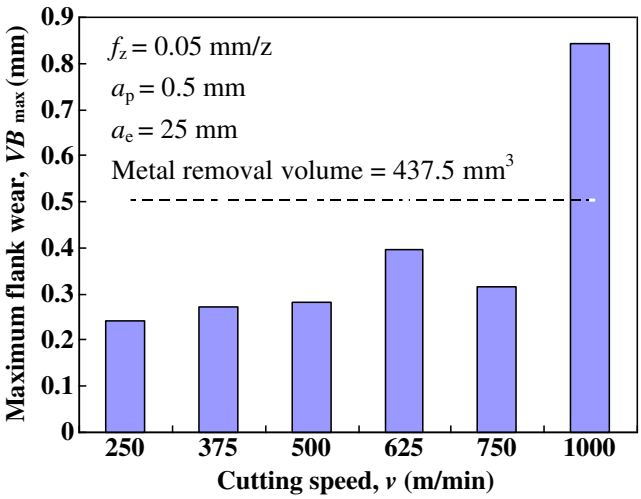

Fig. 3 Flank wear vs. cutting speed in high-speed milling of Ti–6Al–4V alloy with PCD inserts (the thickness of the PCD layer embedded in the insert is 0.5 mm)

3 Results and discussions

3.1 Tool wear and tool failure patterns

Figure 3 shows the maximum flank wear after removing the same metal volume 437.5 mm^3 under different cutting speeds in high-speed face milling of Ti–6Al–4V alloy, tested under coolant condition with 0.05-mm/z feed per tooth, 0.5-mm axial depth of cut, and 25-mm radial depth of cut. As can be seen from Fig. 3, there is a clear increase in the flank wear versus cutting speed for the PCD inserts. The maximum flank wear of the PCD tool at cutting speed of 1,000 m/min even exceeded the thickness of PCD layer (0.5 mm) embedded in the insert, leading to catastrophic failure of the flank face. Thus, the PCD tools are not suitable for machining of Ti–6Al–4V titanium alloy with a cutting speed higher than 1,000 m/min.

Figures 4 and 5 show the wear morphologies of the rake faces and flank faces after removing 437.5-mm^3 metal volume of Ti–6Al–4V alloy in high-speed face milling, respectively. From these figures, the tool wear patterns of the PCD inserts are mainly cutting edge chipping, tool material flaking off the tool rake face, and progressive tool flank wear. The tool wear patters at cutting speed of 250 m/min are slight edge chipping and normal flank wear. However, when the cutting speed exceeded 375 m/min, chunks of tool material flaked off the tool rake face, and the flank wear bands increased remarkably. The serious chipping or flaking should be attributed to the enhanced impacts with the increase in cutting speed in the milling operations. The increased cutting speed increased the cutting force and temperature, and the tool insert worn non-normally because of the limited endurance to strengthened impacts, leading to the tool breakage or damage, such as chipping and flaking. Moreover, notches can be observed at higher cutting speed as shown in Figs. 4 d–f and 5 d–f, the notch wear increase greatly with the further increase in cutting speed.

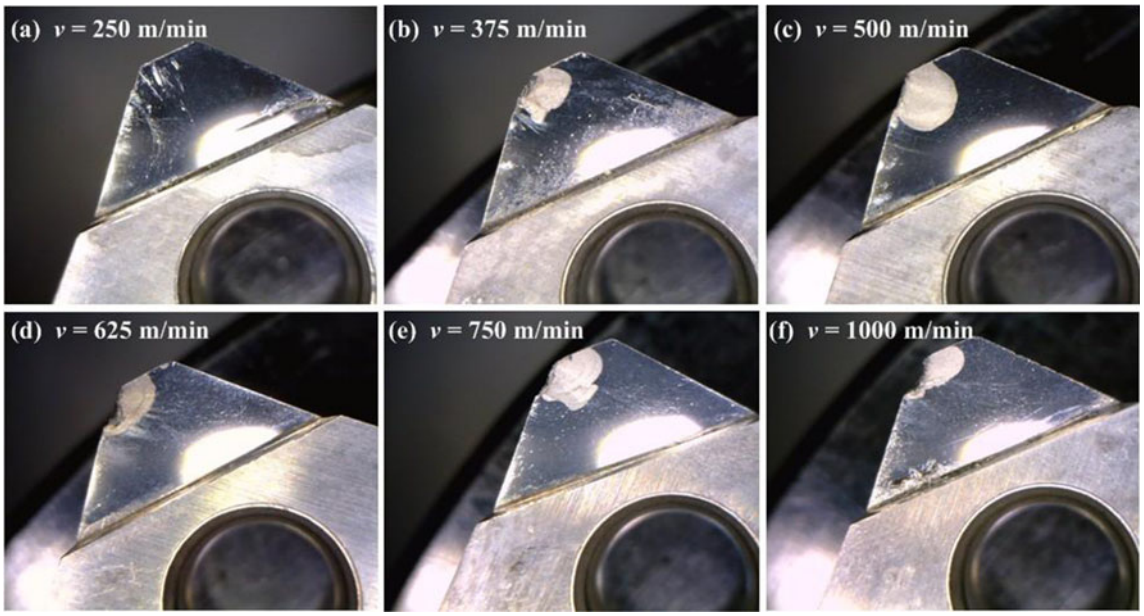

Fig. 4 Rake faces of PCD tools in high-speed milling of Ti–6Al–4V alloy (a_p=0.5 mm, f_z=0.05 mm/z, a_e=25 mm)

3.2 Tool wear mechanisms

PCD tool material possesses low strength and large brittleness, despite its high hardness. The tool is subjected to high cyclic thermal–mechanical impacts in high-speed milling processes, and such large stresses and the cyclic nature of stresses during the intermittent cutting created many voids and cracks, which lead to failure. The large compressive and shear stresses near the cutting tool edge are responsible for edge chipping and spalling of tool materials near the cutting edge on rake face as shown in Figs. 4 and 5.

Figure 6 a shows the SEM image of the PCD tool after machining at cutting peed of 250 m/min, and the EDS chemical composition analyses on the wear track (point A and point B) are illustrated in Fig. 6b and c. Figure 6b illustrates the C element of the PCD and small amount of W and Co elements penetrating from the WC–Co-cemented carbide tool substrate 0.5 mm below the PCD lawyer. Ti, Al,

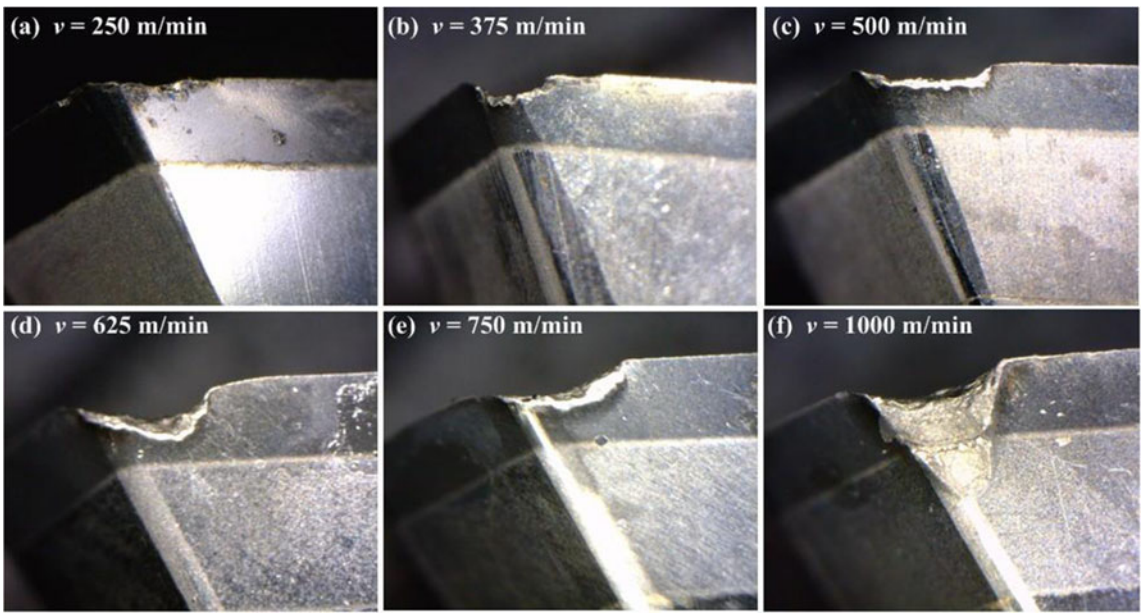

Fig. 5 Flank faces of PCD tools in high-speed milling of Ti–6Al–4V alloy (a_p=0.5 mm, f_z=0.05 mm/z, a_e=25 mm)

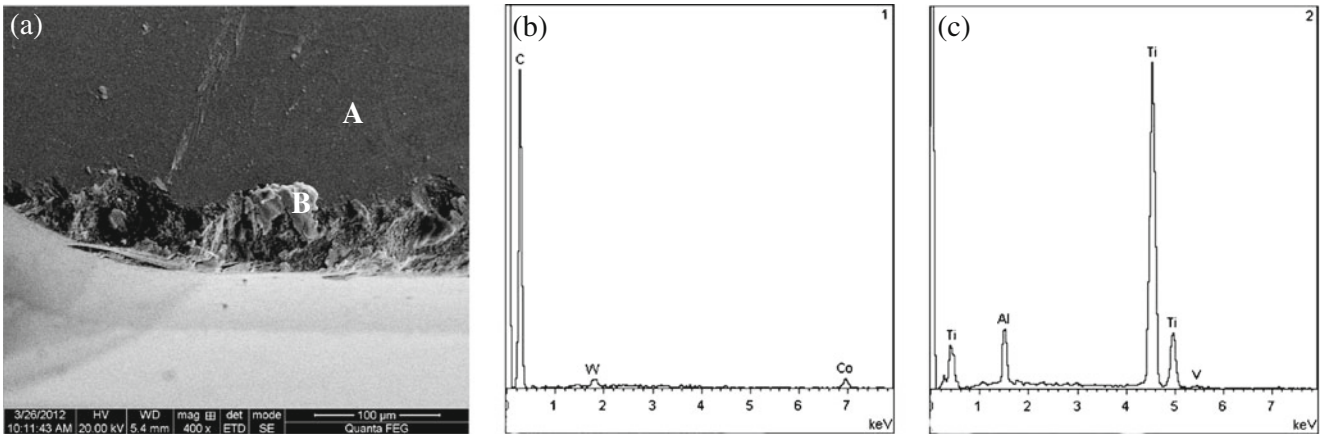

Fig. 6 SEM micrograph of the PCD tool after wet milling of Ti–6Al–4V alloy (v=250 m/min, a_p=0.5 mm, f_z=0.05 mm/z, a_e=25 mm). **a** SEM micrograph of the worn cutting edge, **b** EDS spectrum of the selected area point *A*, **c** EDS spectrum of the selected area point *B*

and V elements were identified in worn area of the cutting edge (Fig. 6c), while the PCD tool contains no Ti, Al, and V elements prior to machining. Apparently, the Ti, Al, and V elements are adhered from the Ti–6Al–4V workpiece materials, and are attached to the tool rake face. It is well-known that the low thermal conductivity of Ti–6Al–4V alloy (6.7 W/(mK)) leads to a localized region of high cutting temperature at the tool-workpiece interface. Titanium chips have a strong tendency to weld to the cutting edge under high cutting temperature, particularly after the tool starts to wear.

The EDS surface maps of scanning analysis results of C, Ti, Al, and V elements for the worn PCD tool in milling of Ti–6Al–4V alloy at cutting peed of 250 m/min are shown in Fig. 7. A significant amount of material adhesion can be observed on both the flank and rake faces of the worn tool. It can be deduced that adhesive wear happened along with progressive abrasion at cutting speed of 250 m/min. Further adhesion may occur on the exposed PCD abrasive surface. The repeated adhering of the workpiece material to the tool and breaking away from the tool after adhesion may initiate the loss of the tool materials from the worn tool face.

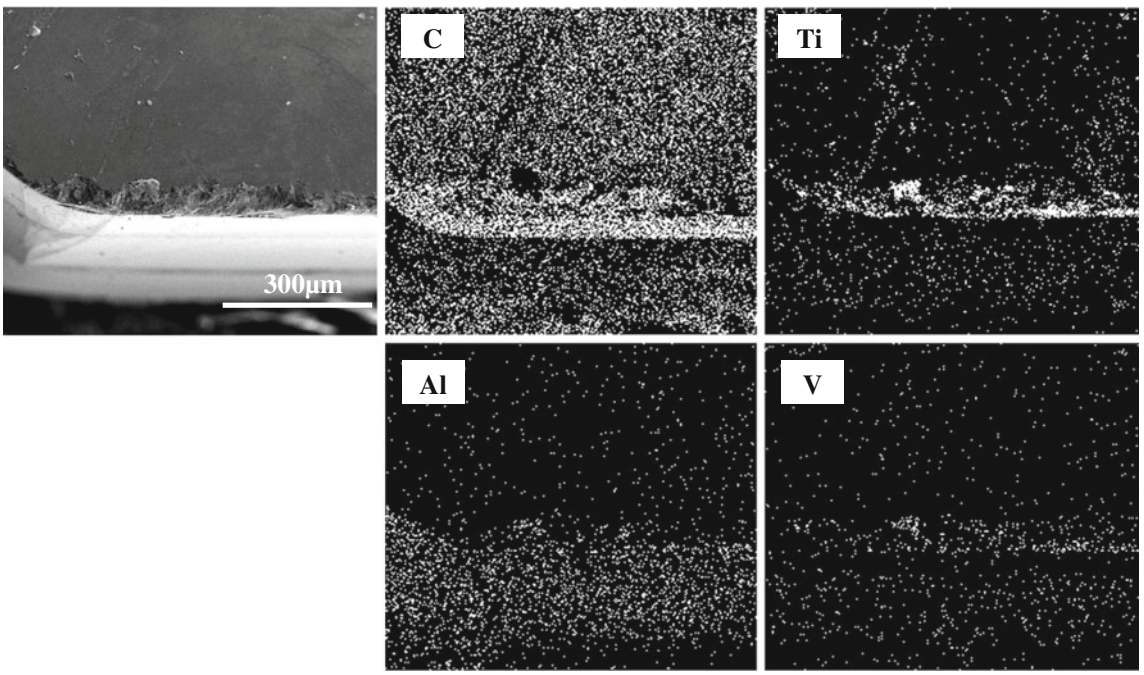

Fig. 7 SEM micrograph of the worn PCD tool after wet milling of Ti–6Al–4V alloy and the corresponding EDS surface maps of scanning analysis results of C, Ti, Al, and V elements. (v=250 m/min, a_p=0.5 mm, f_z=0.05 mm/z, a_e=25 mm)

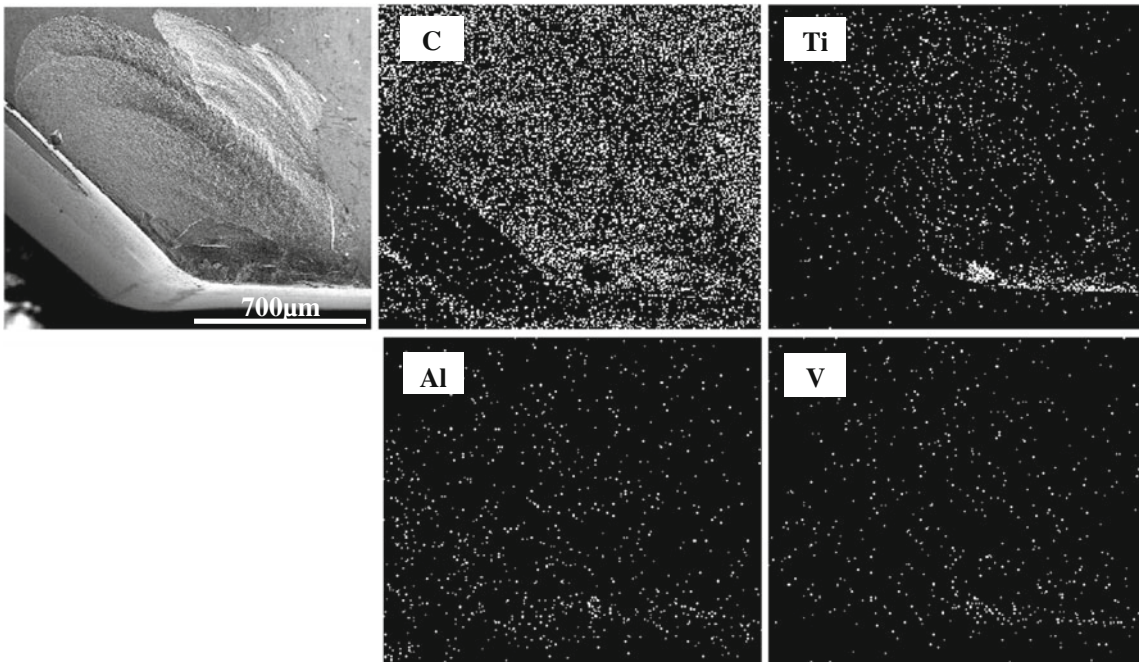

Fig. 8 SEM micrograph of the worn PCD tool after wet milling of Ti–6Al–4V alloy and the corresponding EDS surface maps of scanning analysis results of C, Ti, Al, and V elements. (v=750 m/min, a_p=0.5 mm, f_z=0.05 mm/z, a_e=25 mm)

Figure 8 shows SEM micrograph of the worn PCD tool after wet milling of Ti–6Al–4V alloy and the corresponding EDS surface maps of scanning analysis results of C, Ti, Al, and V elements at cutting speed of 750 m/min. Serious and significant edge chipping and chunks of tool material flaked off the tool rake face can be observed, and this tool wear phenomenon should be attributed to the intense thermal–mechanical impacts under higher cutting speed. A significant amount of material adhesion can be seen along the cutting edge both on the flank and rake faces of the worn tool from the EDS surface maps of scanning analysis results, and there is little material adhesion on the chipped or flaked surface. Figure 9 illustrated the EDS chemical composition analyses on the wear track (point A and point B) after machining at cutting peed of 750 m/min. It also demonstrates that the adhesion was found near the worn cutting edge rather than on the chipping or flaking surface formed under enhanced thermal–mechanical impacts.

The SEM image of the PCD tool after machining at cutting peed of 1,000 m/min and the EDS chemical composition analyses on the wear track (points E and F) are shown in Fig. 10. A notch at the limit of the cutting zone is

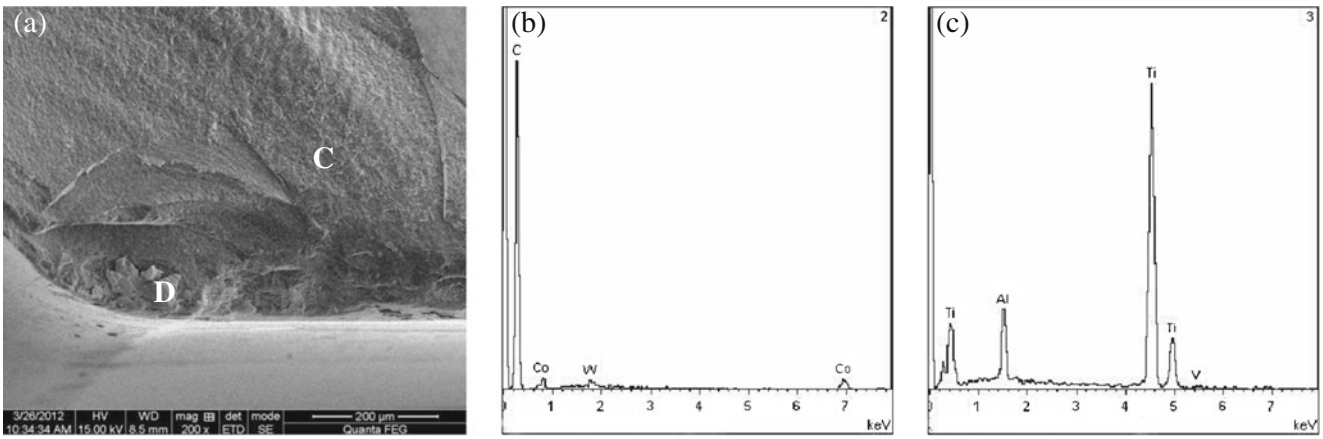

Fig. 9 SEM micrograph of the PCD tool after wet milling of Ti–6Al–4V alloy (v=750 m/min, a_p=0.5 mm, f_z=0.05 mm/z, a_e=25 mm). **a** SEM micrograph of the worn cutting edge, **b** EDS spectrum of the selected area point *C*, **c** EDS spectrum of the selected area point *D*

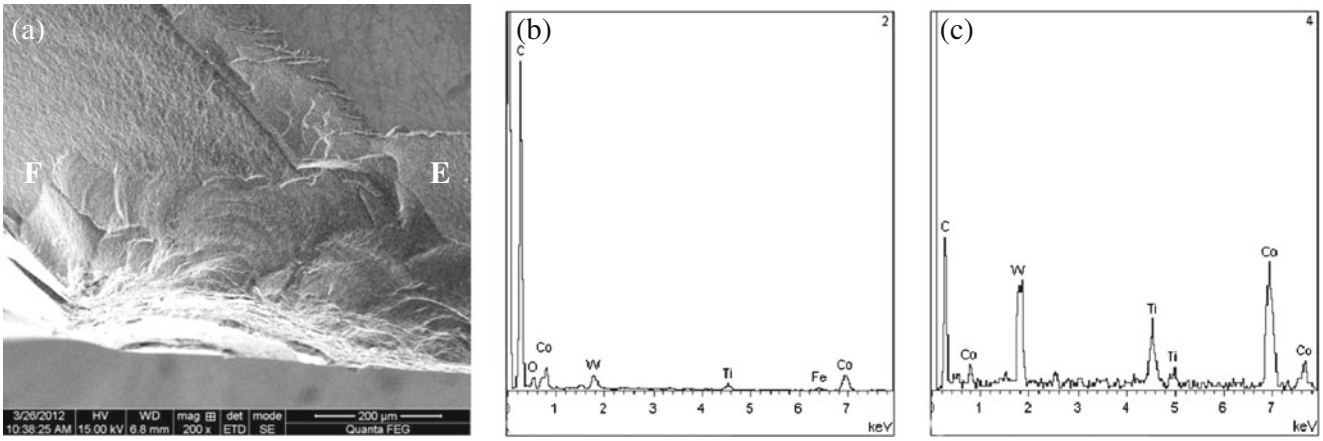

Fig. 10 SEM micrograph of the PCD tool after wet milling of Ti–6Al–4V alloy (v=1,000 m/min, a_p=0.5 mm, f_z=0.05 mm/z, a_e=25 mm). **a** SEM micrograph of the worn cutting edge, **b** EDS spectrum of the selected area point *E*, **c** EDS spectrum of the selected area point *F*

observed in Fig. 10 a. Notch wear was caused by the high cutting temperature a few millimeters from the tool nose, and these high temperatures are explained by the low thermal conductivity and high heat capacity of Ti–6Al–4V alloy related to the very high thermal conductivity of the PCD tool (550 W/mK) [12]. From the results of the EDS analysis of point E, O element was observed (Fig. 10 b). Under high cutting speed, the Ti–6Al–4V chips easily burn immediately after leaving off the tool face, so it can be inferred that chemical reactions severely happen during the cutting process. It is the evident of oxidation wear. Compared with the EDS analysis results of selected area point C at cutting speed of 750 m/min (Fig. 9 b), oxidation wear was convinced to be happening at cutting speed of 1,000 m/min.

4 Conclusions

A series of milling tests in the high cutting speed ranges were conducted to better understand the wear mechanisms associated with PCD tools. The following conclusions were drawn:

1. Cutting speeds were found to have a profound effect on the wear behaviors of PCD tools. The PCD tools exhibited relative small edge chipping and flank wear at cutting speed of 250 m/min, within further increasing of the cutting speed the flank wear and breakage increased greatly. Cutting speeds around 250 m/min were proved to be the best range for PCD tools when machining Ti–6Al–4V titanium alloy.
2. Breakage at take face was found to be the predominant failure mechanism when milling Ti–6Al–4V titanium alloy at cutting speed higher than 375 m/min. While the mechanisms responsible for tool materials flaking off the tool rake face were determined to be the enhanced thermal–mechanical impacts with the increase in cutting speed in the intermittent cutting operations.
3. Adhesion was found on the worn rake face and flank face near the cutting edge rather than on the chipped or flaked surface on the rake face.
4. The failure mechanisms of PCD tools in high-speed wet milling of Ti–6Al–4V titanium alloy were mainly premature breakage and synergistic interaction among adhesive wear and abrasive wear.

Acknowledgments This work is sponsored by the National Basic Research Program of China (2009CB724402), the National Natural Science Foundation of China (51175310), and the Graduate Innovation Foundation of Shandong University (yyx10012).

References

1. Ezugwu EO, Wang ZM (1997) Titanium alloys and their machinability—a review. J Mater Process Technol 68(3):262–274
2. Ezugwu EO, Bonney J, Yamane Y (2003) An overview of the machinability of aeroengine alloys. J Mater Process Technol 134 (2):233–253
3. Li R, Shih AJ (2006) Finite element modeling of 3D turning of titanium. Int J Adv Manuf Technol 29(3–4):253–261
4. Li AH, Zhao J, Zhou YH, Chen XX, Wang D (2012) Experimental investigation on chip morphologies in high-speed dry milling of titanium alloy Ti–6Al–4V. Int J Adv Manuf Technol 62(9–12):933–942
5. Li AH, Zhao J, Luo HB, Zheng W (2011) Machined surface analysis in high-speed dry milling of Ti–6Al–4V alloy with coated carbide inserts. Adv Mater Res 325:412–417
6. Li AH, Zhao J, Luo HB, Pei ZQ, Wang ZM (2012) Progressive tool failure in high-speed dry milling of Ti–6Al–4V alloy with coated carbide tools. Int J Adv Manuf Technol 58(5–8):465–478

7. Li AH, Zhao J, Luo HB, Pei ZQ (2012) Wear mechanisms of coated carbide tools in high-speed dry milling of titanium alloy. Tribology 32(1):40–46
8. Jawaid A, Sharif S, Koksal S (2000) Evaluation of wear mechanisms of coated carbide tools when face milling titanium alloy. J Mater Process Technol 99(1–3):266–274
9. De Melo ACA, Milan JCG, Da Silva MD, Machado AR (2006) Some observation on wear and damages in cemented carbide tools. J Braz Soc Mech Sci Eng 28(3):269–277
10. Deng JX, Li YS, Song WL (2008) Diffusion wear in dry cutting of Ti–6Al–4V with WC/Co carbide tools. Wear 265(11–12):1776–1783
11. Wu Z, Deng JX, Chen Y, Xing YQ, Zhao J (2012) Performance of the self-lubricating textured tools in dry cutting of Ti–6Al–4V. Int J Adv Manuf Technol 62(9–12):943–951
12. Corduan N, Himbart T, Poulachon G, Dessoly M, Lambertin M, Vigneau J, Payoux B (2003) Wear mechanisms of new tool materials for Ti–6AI–4V high performance machining. CIRP Ann Manuf Technol 52(1):73–76
13. Li AH, Zhao J, Wang D, Gao XL, Tang HW (2013) Three-point bending fatigue behavior of WC–Co cemented carbides. Mater Des 45:271–278
14. Nurul Amin AKM, Ismail AF, Nor Khairusshima MK (2007) Effectiveness of uncoated WC–Co and PCD inserts in end milling of titanium alloy—Ti–6Al–4V. J Mater Process Technol 192–193:147–158
15. Heath PJ (2001) Developments in applications of PCD tooling. J Mater Process Technol 116(1):31–38
16. Nabhani F (2001) Wear mechanisms of ultra-hard cutting tools materials. J Mater Process Technol 115(3):402–412
17. Oosthuizen GA, Akdogan G, Treurnicht N (2011) The performance of PCD tools in high-speed milling of Ti6Al4V. Int J Adv Manuf Technol 52(9–12):929–935